PCP
PLANT & CELL PHYSIOLOGY

In Planta Processing of the SpCas9–gRNA Complex

Masafumi Mikami[1,2], Seiichi Toki[1,2,3] and Masaki Endo[2,*]

[1]Graduate School of Nanobioscience, Yokohama City University, 22- 2 Seto, Yokohama, Kanagawa 236-0027, Japan
[2]Plant Genome Engineering Research Unit, Institute of Agrobiological Sciences, National Agriculture and Food Research Organization, 2-1-2 Kannondai, Tsukuba, Ibaraki 305-8602, Japan
[3]Kihara Institute for Biological Research, Yokohama City University, 641-12 Maioka-cho, Yokohama, Kanagawa 244-0813, Japan
*Corresponding author, E-mail, mendo@affrc.go.jp; Fax, +81-29-838-8450.
(Received August 7, 2017; Accepted October 9, 2017)

Rapid Paper

In CRISPR/Cas9 (clustered regularly interspaced short palindromic repeat/CRISPR-associated protein 9)-mediated genome editing in plants, *Streptococcus pyogenes* Cas9 (SpCas9) protein and the required guide RNA (gRNA) are, in most cases, expressed from a stably integrated transgene. Generally, SpCas9 protein is expressed from an RNA polymerase (pol) II promoter, while gRNA is expressed from a pol III promoter. However, pol III promoters have not been much characterized other than in model plants, making it difficult to select appropriate promoters for specific applications, while pol II transcripts have to be processed to generate functional gRNAs. Recently, successful processing of a pol II transcript into functional gRNAs using ribozyme or Csy4-RNA cleavage systems has been demonstrated. Here, we show that functional gRNAs can be efficiently processed using SpCas9 protein and plant endogenous RNA cleavage systems without the need for a specific RNA processing system. In our system, SpCas9 RNA and gRNA are both transcribed as a single RNA using a single pol II promoter; translated SpCas9 protein can be bound to this RNA and, finally, extra RNA sequences are trimmed by plant RNA processing systems to form a functional SpCas9–gRNA complex. The efficiency of targeted mutagenesis using our novel SpCas9–gRNA fused system was comparable with that of the SpCas9–gRNA system with ribozyme sequence, achieving rates of up to 100% in rice. Our results could be useful in developing stable SpCas9–gRNA expression systems and in RNA virus vector-mediated genome editing systems in plants.

Keywords: CRISPR/Cas9 • Ribozyme • Targeted mutagenesis.

Abbreviations: CaMV, *Cauliflower mosaic virus*; CAPS, cleaved amplified polymorphic sequence; Cas9, CRISPR-associated protein 9; CRISPR, clustered regularly interspaced short palindromic repeat; crRNA, CRISPR RNA; DL, *DROOPING LEAF*; DMC1A, *DISRUPTED MEIOTIC cDNA 1 A*; GFP, green fluorescent protein; gRNA, guide RNA; HPT, HYGROMYCIN, PHOSPHOTRANSFERASE; PAM, protospacer adjacent motif; PDS, *PHYTOENE DESATURASE*; pol, RNA polymerase; RGR, ribozyme–gRNA–ribozyme; tracrRNA, *trans*-activating CRISPR RNA; YSA, *YOUNG SEEDLING ALBINO*.

Introduction

Recent years have seen an explosion in the use of CRISPR (clustered regularly interspaced short palindromic repeats)/Cas9 (CRISPR-associated protein 9) as a genome editing tool in various organisms, including bacteria, yeast, animals and plants (Jinek et al. 2012, Cho et al. 2013, Cong et al. 2013, DiCarlo et al. 2013, Hwang et al. 2013, Jiang et al. 2013, Jinek et al. 2013, Bortesi and Fischer 2015, Ma et al. 2016). The CRISPR/Cas9 system requires two elements: (i) a Cas9 protein containing a nuclease domain, expressed from an RNA polymerase II (pol II) promoter that can drive tissue-specific or inducible gene expression; and (ii) a guide RNA (gRNA) that provides sequence specificity to the target DNA and is expressed from an RNA polymerase III (pol III) promoter that usually drives the ubiquitous expression of this small RNA in all tissues. However, the pol III promoters of many organisms have not been characterized, making it difficult to choose appropriate promoters for CRISPR/Cas9-mediated targeted mutagenesis. Thus, pol III promoters such as those of the U6 small nuclear RNA gene from *Arabidopsis thaliana* or rice (AtU6-26 or OsU6-2, respectively) are often chosen to express gRNAs because these promoters are among the few known to be suitable for the transcription of small RNAs (Li et al. 2013, Nekrasov et al. 2013, Shan et al. 2013, Bortesi and Fischer 2015).

Extra nucleotides added to the 5′ and 3′ end of a gRNA have a negative effect on gRNA function (Hsu et al. 2013, Mali et al. 2013). Thus, the expression of multi-gRNAs from a single pol II promoter requires RNA processing of primary transcripts to form independent functional gRNAs. Among the processing machineries used to generate functional gRNAs, there have been several reports of successful CRISPR/Cas9-mediated targeted mutagenesis using ribozyme, Csy4 and tRNA processing systems (Raitskin and Patron 2015, Lowder et al. 2016, Schwartz et al. 2016). Gao et al. reported CRISPR/Cas9-mediated targeted mutagenesis using a ribozyme–gRNA–ribozyme (RGR) system in yeast and Arabidopsis (Gao and Zhao 2014, Gao et al. 2015). In the RGR system, the gRNA (driven by a pol II promoter) was processed by site-specific self-cleavage of the ribozyme, creating a functional gRNA. Using the RGR system, Yoshioka et al. (2015) reported a mono-promoter-driven CRISPR/Cas9 system in

Plant Cell Physiol. 58(11): 1857–1867 (2017) doi:10.1093/pcp/pcx154, Advance Access publication on 12 October 2017, available online at www.pcp.oxfordjournals.org

mammalian cells (Yoshioka et al. 2015). Recently, a single transcript unit (STU) CRISPR/Cas9 system using the hammerhead ribozyme was reported for CRISPR/Cas9 expression in plants (Tang et al. 2016), while gRNAs transcribed by a pol II promoter can be processed by the Csy4 endoribonuclease RNA cleavage system in mammalian cells (Nissim et al. 2014). The Csy4 processing system utilizes the CRISPR type III RNase, Csy4, to cleave the 20 bp sequences that flank the gRNAs (Haurwitz et al. 2010, Tsai et al. 2014). Recently, successful CRISPR/Cas9-mediated targeted mutagenesis using the Csy4 processing system in plants has been reported (Cermak et al. 2017). Furthermore, Xie et al. (2015) reported the use of the polycistronic tRNA–gRNA (PTG) gene system to produce multiplex gRNAs from a single transcript in plants (Xie et al. 2015, Minkenberg et al. 2016). In this system, the endogeneous RNase P and RNase Z cleave tRNA precursors to remove extra 5′ and 3′ sequences, respectively (Schiffer et al. 2002, Barbezier et al. 2009, Canino et al. 2009, Phizicky and Hopper 2010, Gutmann et al. 2012). Recently, Cermak et al. (2017) reported that Csy4 and tRNA processing systems using the *Cestrum yellow leaf curling virus* (CmYLCV) promoter as a pol II promoter are almost twice as effective in inducing mutations as gRNAs expressed from individual pol III promoters in plants (Cermak et al. 2017). Thus, using pol II promoters to express gRNAs can improve CRISPR/Cas9-meditaed targeted mutagenesis efficiency compared with using pol III promoters. However, in ribozyme, Csy4 and tRNA processing devices, specific sequences are required for processing individual functional gRNAs (i.e. ribozyme cleavage sites are 15 or 43 bp, Csy4 recognition sites are 20 bp and tRNA recognition sites are 77 bp).

To simplify and miniaturize the Cas9–gRNA expression construct, in the present study we designed a SpCas9 (*Streptococcus pyogenes* Cas9)–gRNA expression construct in which both SpCas9 and gRNAs were driven by a single pol II promoter without ribozyme sequences, and evaluated mutation efficiency in rice and Arabidopsis using this system.

Results

Targeted mutagenesis using SpCas9–gRNA vector with or without ribozyme sequences

We designed two vectors expressing both the *SpCas9* gene (optimized for rice codon usage; Mikami et al. 2015) and a gRNA under a single pol II promoter [the maize polyubiquitin-1 gene promoter (ZmUbi); Takimoto et al. 1994], to create two vectors, in which the gRNA is connected to the 3′ end of the *SpCas9* gene with [SpCas9–ribozyme (rz)–gRNA] or without (SpCas9–gRNA) the hammerhead ribozyme sequence (**Fig. 1A**). These constructs were introduced separately into rice calli via *Agrobacterium*-mediated transformation, and mutation frequency was assessed using the target gene *DROOPING LEAF* (*DL*) (Yamaguchi et al. 2004). CAPS (cleaved amplified polymorphic sequence) analysis revealed induced mutations at the gDL-1 locus (PCR products remain undigested by a restriction enzyme with a recognition site at the target locus; **Fig. 1B**). Using construct SpCas9–rz–gRNA, mutations at the gDL-1 locus were detected in most calli (11/12 lines; **Fig. 1B**, upper panel). To estimate the mutation frequency in independent transgenic calli, PCR products derived from independent calli were cloned into plasmids and sequenced. This analysis revealed that mutation at the gDL-1 locus was achieved with high efficiency (up to 100% in callus line number #4; **Fig. 1B**, upper panel). Similar results were obtained in calli transformed with the SpCas9–gRNA construct; mutation frequencies in calli lines #1 and #9 were 85% and 87.5%, respectively (**Fig. 1B**, lower panel). We examined the patterns of mutation induced by these constructs at the gDL-1 locus (**Fig. 1C**; Supplementary Fig. S1A). Regardless of the presence or absence of the hammerhead ribozyme sequence, small deletions or small insertions around the protospacer adjacent motif (PAM) sequence were often induced by both vectors (**Fig. 1C**; Supplementary Fig. S1A). Targeted mutagenesis using both constructs was also observed with high efficiently in other target genes, for example the *YOUNG SEEDLING ALBINO* (*YSA*) and *PHYTOENE DESATURASE* (*PDS*) genes, and other target sequences in the *DL* gene (Supplementary Fig. S1B). Furthermore, targeted mutagenesis using SpCas9–rz–gRNA or SpCas9–gRNA vectors harboring the *SpCas9* gene optimized for Arabidopsis codon usage (Fauser et al. 2014) was also successful in Arabidopsis (Supplementary Fig. S2). Because the targeted mutation efficiency of the SpCas9–gRNA vector was comparable with that of the SpCas9–rz–gRNA vector in plants, we concluded that the ribozyme sequence is not necessary for generating functional gRNAs.

Targeted mutagenesis using a gRNA driven by the 2 × 35S promoter

As a control experiment of gRNA expression from a pol II promoter, we designed the vector SpCas9/2 × 35SgRNA (**Fig. 2A**). In this vector, the *SpCas9* gene was driven by the ZmUbi promoter and the gRNA was under the control of the 2 × 35S promoter. The gRNA generated from calli transformed with the SpCas9/2 × 35SgRNA construct might have a 5′-cap structure and 3′-poly(A) tail sequence (**Fig. 2A**). We confirmed that mutations were induced in SpCas9/2 × 35SgRNA vector-transformed calli, and that targeted mutagenesis at the gDL-1 locus was observed with high efficiency (up to 100% in line #6; **Fig. 2B**, upper left). The same result was obtained in another target gene, *DISRUPTED MEIOTIC cDNA 1 A* (*DMC1A*; Sakane et al. 2008; **Fig. 2B**, lower left). The efficiency of targeted mutagenesis using SpCas9/2 × 35SgRNA vector was comparable with that using the vector SpCas9/OsU6gRNA (**Fig. 2B**).

gRNA transcripts in SpCas9–gRNA vector-transformed rice calli

To investigate transcripts of SpCas9–rz–gRNA- and SpCas9–gRNA-transformed calli, Northern blot analysis of gRNA was conducted using total RNA extracted from transgenic calli. A schematic representation of the expected gRNA structures is shown in **Fig. 3A**. The expected sizes of the gRNA using SpCas9/OsU6gRNA and SpCas9/2 × 35SgRNA vectors are 104 nucleotides (nt) and 259 nt without the 3′-poly(A) tail sequence,

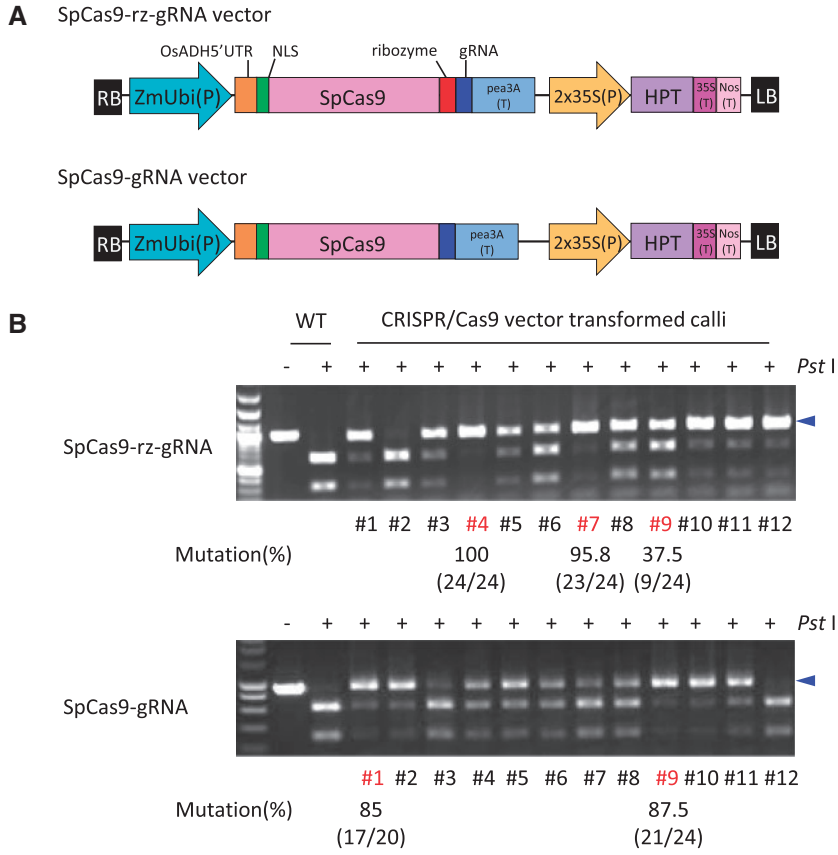

Fig. 1 Targeted mutagenesis using SpCas9–rz–gRNA or SpCas9–gRNA systems in rice calli. (A) Schematic representation of SpCas9–rz–gRNA and SpCas9–gRNA vectors. (B) CAPS analysis of the *DL* gene in SpCas9–rz–gRNA vector-transformed calli and SpCas9–gRNA vector-transformed calli. The mutation frequency of calli (shown in red) was calculated from the ratio of sequenced clones with mutation. –, non-digested PCR products; +, *Pst* I-digested PCR products. A blue arrowhead indicates the position of undigested PCR products. An undigested band indicates mutations in the target loci. (C) Mutation variations in the target site in SpCas9–gRNA vector-transformed callus line #9. The wild-type sequence is shown at the top, with the PAM sequence in green and the 20 nt target sequence in red. The blue arrowhead indicates the expected cleavage site. Dashes, deleted bases. The net changes in length are shown to the right of each sequence (+, insertion; –, deletion). The number of clones representing each mutant allele is shown in parentheses.

respectively (detailed sequences are shown in Supplementary Fig. S3A). The expected size of full-length RNA of SpCas9–rz–gRNA is 4,497 nt without the 3′-poly(A) tail sequence, and the gRNA processed by ribozyme from full-length RNA is 332 nt (**Fig. 3A**; Supplementary Fig. S3B). In Northern blot analysis using a probe on the scaffold sequence of the gRNA, the expected bands appeared in OsU6gRNA-transformed calli (**Fig. 3B**, band *a*). On the other hand, the size of the band detected in 2 × 35SgRNA (band *b*) was larger than the expected 259 nt, and close to the 310 nt band of marker-1 (**Figs. 3B**, **4D**). Since a 3′-poly(A) tail sequence could have been added to 2 × 35SgRNA, band *b* seems to be the full-length transcribed RNA of 2 × 35SgRNA with a 3′-poly(A) tail.

In calli transformed with the SpCas9–rz–gRNA vector, two bands were detected (**Fig. 3B**, bands *c* and *d*). Band *c* was approximately 400 nt, corresponding to the expected size of the gRNA processed by ribozyme from the full-length RNA of the SpCas9–rz–gRNA construct (**Fig. 3A**), whereas band *d* of approximately 100 nt was unexpected (**Fig. 3B**; Supplementary Fig. S4). Because mutations were detected in SpCas9–rz–

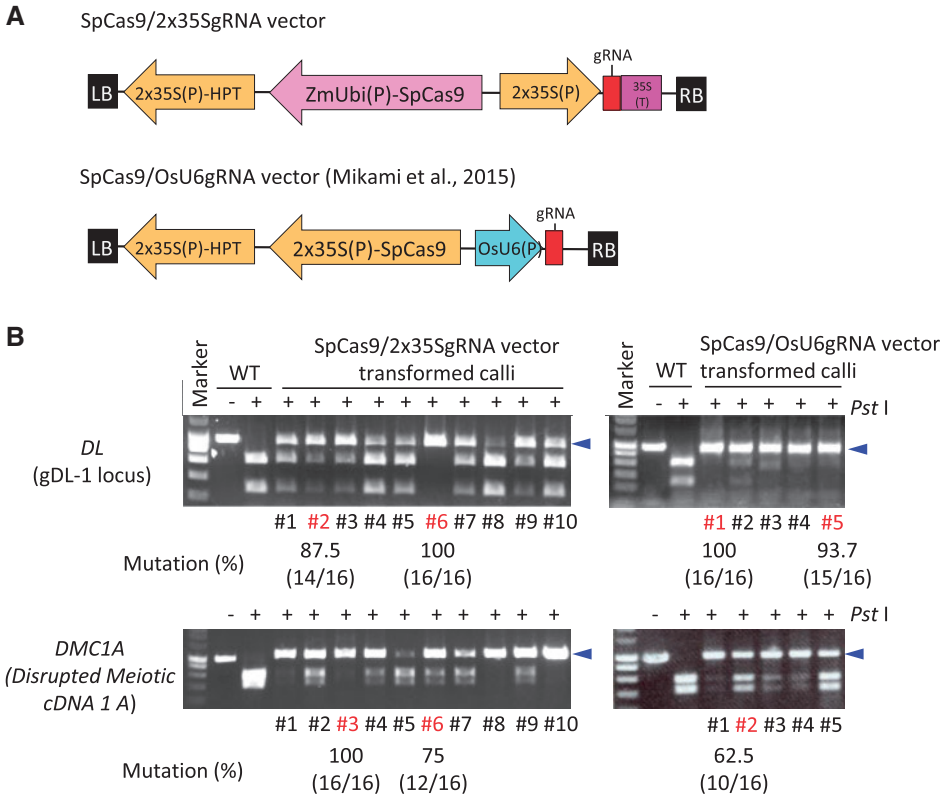

Fig. 2 Targeted mutagenesis using the SpCas9/2 × 35SgRNA vector in rice calli. (A) Schematic representation of the constructs used in this study. (B) CAPS analysis of *DL* and *DMC1A* genes in SpCas9/2 × 35SgRNA and SpCas9/OsU6gRNA vector-transformed calli. The mutation frequency of calli (shown in red) was calculated from the ratio of sequenced clones with mutation. –, non-digested PCR products; +, *Pst* I-digested PCR products. A blue arrowhead indicates the position of undigested PCR products. An undigested band indicates mutations in the target loci.

gRNA vector-transformed calli (**Fig. 1B**, upper panel), the gRNAs detected as bands *c* and/or *d* must have been functional. Futhermore, two bands were also detected in SpCas9–gRNA vector-transformed calli at the same position (**Fig. 3B**), despite the fact that this vector does not contain the ribozyme sequence. This result indicates that there is a gRNA processing mechanism for generating a functional gRNA in rice, even when the ribozyme sequence is absent. The gRNA expression level differed depending on the promoters used [the 2 × 35S promoter, the ZmUbi promoter (Takimoto et al. 1994), the ubiquitin 4-2 promoter from *Petroselinum crispum* (Fauser et al. 2012) (PcUbi) and the synthetic promoter (Ishige et al. 1999) (G10-90)], but gRNA band patterns were always the same (**Fig. 3B**). Both the mutation frequency (**Fig. 1B**; Supplementary Fig. S5) and the gRNA transcript level (**Fig. 3B**) were highest when the ZmUbi promoter was used to drive the SpCas9 and gRNA unit. The efficiency of targeted mutagenesis seems to be linearly correlated with the expression level of SpCas9 and gRNA under the single pol II promoter.

SpCas9 protein is involved in processing of functional gRNAs in plants

In the CRISPR/Cas9 system of bacteria and archaea, Cas9 protein, *trans*-activating CRISPR RNA (tracrRNA) and endoribonuclease III (RNase III) are involved in the first pre-mRNA processing event (Deltcheva et al. 2011, Chylinski et al. 2013). The duplex RNAs of the CRISPR precursor transcript (pre-crRNA) and tracrRNA are stabilized by the Cas9 protein, and are recognized and cleaved by RNase III (Deltcheva et al. 2011, Charpentier et al. 2015). Because it is not random degradation but rather cleavage at a specific site that seems to occur in the primary transcript of the SpCas9–gRNA, we expected that a similar primary transcript processing system was at work in transgenic rice calli. To investigate whether a SpCas9-dependent gRNA processing (editing) mechanism exists in rice, we designed two vectors, SpCas9/*HYGROMYCIN PHOSPHO TRANSFERASE (HPT)*–rz–gRNA and GFP/HPT–rz–gRNA (**Fig. 4A**). The 2 × 35S::HPT–rz–gRNA::35S:Nos cassette is common to both vectors, but the GFP/HPT–rz–gRNA vector has a green fluorescent protein (GFP) expression cassette instead of the SpCas9 expression cassette. Targeted mutations were efficiently induced in calli transformed with the SpCas9/HPT–rz–gRNA vector (mutation frequency 93.7% in line #2), but not in calli transformed with the GFP/HPT–rz–gRNA vector (**Fig. 4B**). In both vectors, the expected size of full-length RNA of the HPT–rz–gRNA is 1,413 nt without including the 3′-poly(A) tail sequence, and the gRNA processed by ribozyme is 258 nt (**Fig. 4C**; Supplementary Fig. S3C). Three major bands of gRNA were detected in the SpCas9/HPT–rz–gRNA vector-transformed calli (**Fig. 4D**, bands *e*, *f* and *g*). Bands *e* and *f* corresponded to the expected sizes of full-length RNA of HPT–rz–gRNA and the gRNA processed by ribozyme, respectively (**Fig. 4D**). Band *g* was unknown and the size of band *g* was similar to that of

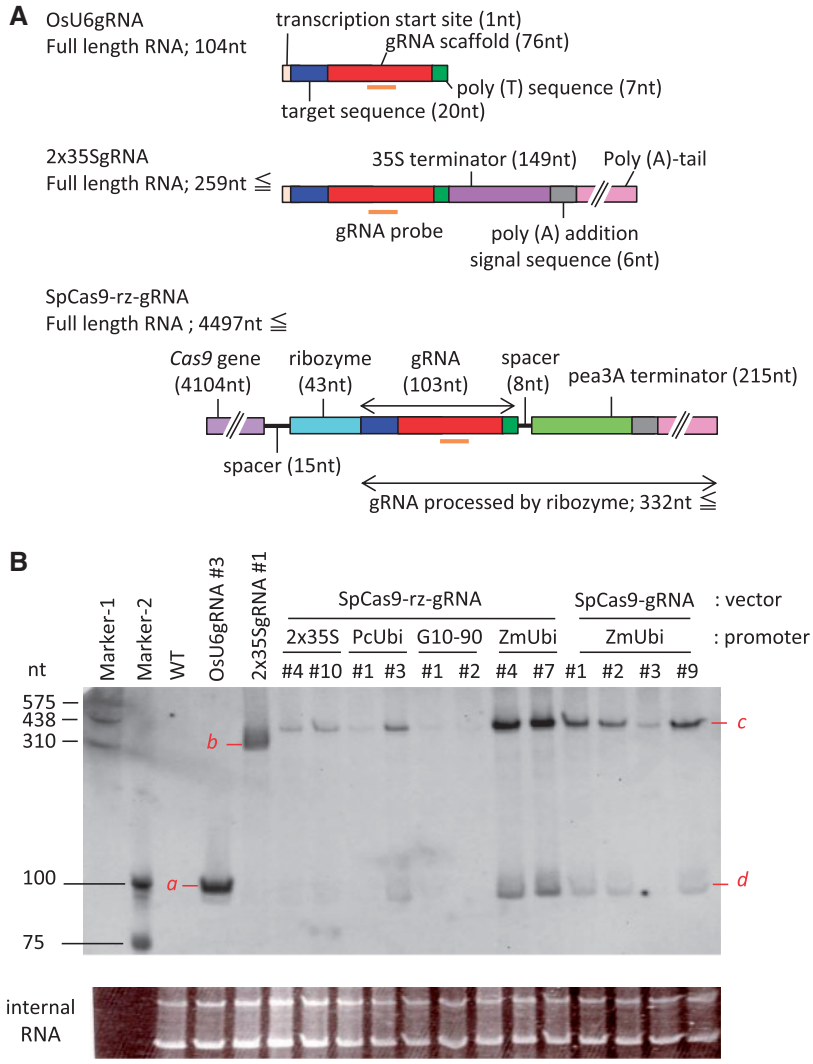

Fig. 3 Northern blot analysis of gRNA expressed in rice calli. (A) Expected structure and size (nt) of gRNAs expressed in rice. (B) Northern blot analysis of total RNA using a probe corresponding to the scaffold sequence of the gRNA. Callus line numbers (e.g. #1) are shown under each promoter name.

band *d* detected in both SpCas9–rz–gRNA and SpCas9–gRNA vector-transformed calli (**Fig. 3B**, band *d*; **Fig. 4D**, band *g*). On the other hand, a single band similar to band *e* was detected in GFP/HPT–gRNA vector-transformed calli (**Fig. 4D**). Despite the presence of ribozyme sequence in the GFP/HPT–gRNA vector-transformed calli, band *f* was not detected. These results indicate that, in plants, the contribution of SpCas9 in gRNA processing is greater than that of the ribozyme sequence.

RNases promote the generation of functional gRNAs in vitro

In the CRISPR/Cas9 system of bacteria and archaea, endogenous RNase III is recruited to cleave tracrRNA and pre-crRNA upon base pairing (Deltcheva et al. 2011, Chylinski et al. 2013). Because Cas9 protein had no RNase III-like motifs (Nicholson 1999, Drider and Condon 2004, Condon 2007), we hypothesized that plant endogenous RNases are recruited to process functional gRNAs from the primary transcript containing the gRNA sequence. First, to demonstrate that non-processed gRNA has no gRNA activity, we prepared five in vitro transcribed gRNAs, OsU6gRNA_T7, 2 × 35SgRNA_T7, SpCas9:fra-rz–gRNA, SpCas9:fra–gRNA and HPT–rz–gRNA_T7 (Supplementary Fig. S6, Nos. 1–5). We found that the hammerhead ribozyme sequence we used was functional for the cleavage of RNA, and bands expected by self-processing of ribozyme were detected in vitro (Supplementary Fig. S7A, bands *h* and *i*; lane Nos. 3 and 5). Regardless of the presence or absence of the SpCas9 protein, a band similar in size to band *i* was not detected in the RNA of the SpCas9:fra–gRNA (Supplementary Fig. S7A, lane No. 4), and the small bands (~103 nt) detected in transgenic calli of vectors SpCas9–gRNA, SpCas9–rz–gRNA and SpCas9/HPT–rz–gRNA (**Fig. 3B**, band *d*; **Fig. 4D**, band *g*) were not detected in in vitro transcribed RNAs of Cas9:fra–rz–gRNA and Cas9:fra–gRNA (Supplementary Fig. S7A). Moreover, in the presence of SpCas9 protein, RNAs of OsU6gRNA_T7, 2 × 35SgRNA_T7, SpCas9:fra–rz–gRNA and HPT–rz–gRN_T7 were able to cleave the linear target DNA efficiently, whereas DNA cleavage was barely induced by the RNA of SpCas9:fra–gRNA and SpCas9

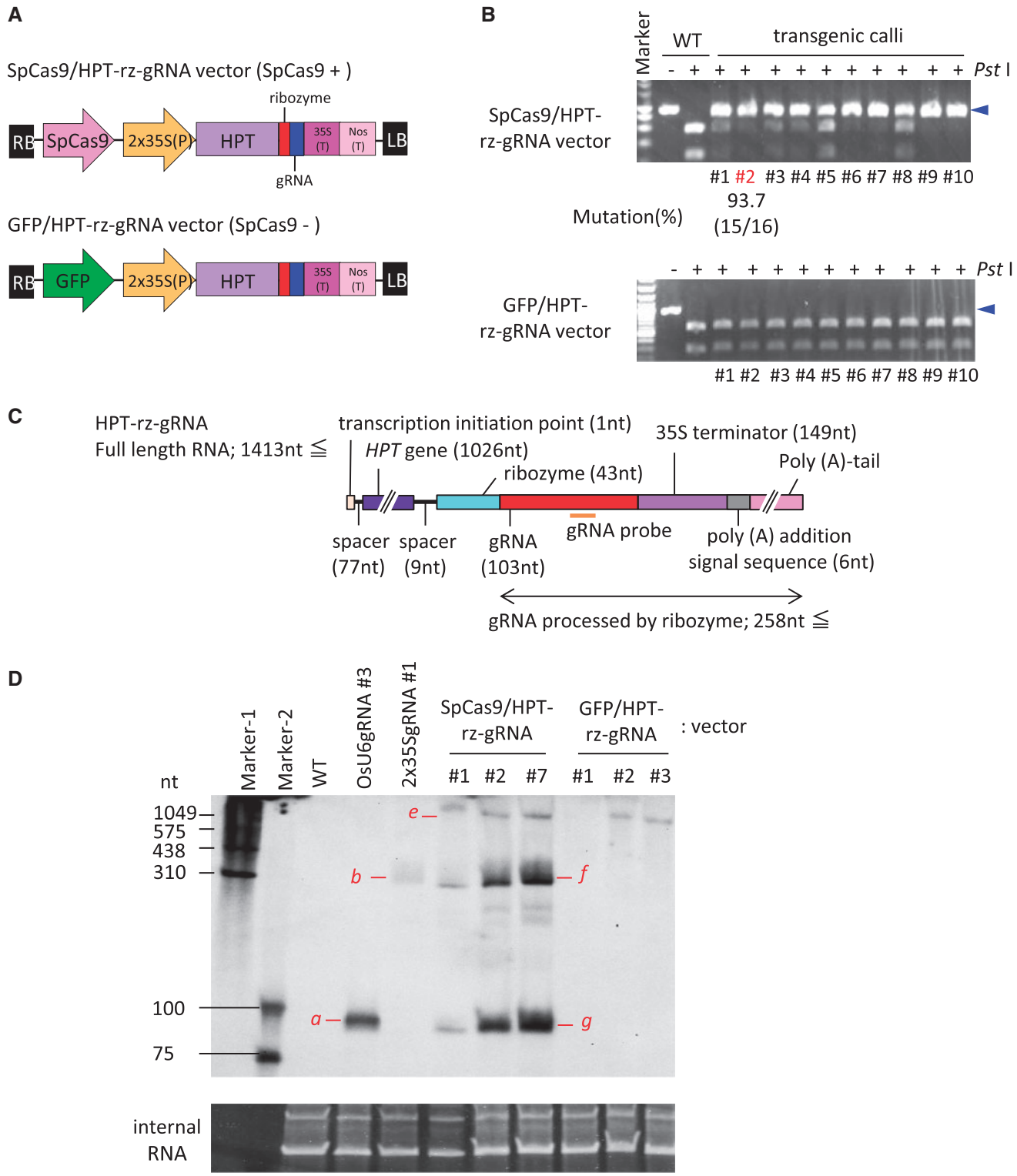

Fig. 4 Analysis of gRNA processing in rice calli with/without SpCas9 expression. (A) Schematic representation of the constructs used in this study. (B) CAPS analysis of the *DL* gene in SpCas9/HPT–rz–gRNA and GFP/HPT–rz–gRNA vector-transformed calli. The mutation frequency of calli (shown in red) was calculated from the ratio of sequenced clones with mutation. –, non-digested PCR products; +, *Pst* I-digested PCR products. A blue arrowhead indicates the position of undigested PCR products. An undigested band indicates mutations in the target loci. (C) Expected structure and size (nt) of gRNA expression using the GFP/HPT–rz–gRNA vector in rice. (D) Northern blot analysis of gRNA in the presence or absence of SpCas9 expression. Callus line numbers (e.g. #1) are shown beneath each vector name.

protein in vitro (Supplementary Fig. S7B). These results show that the presence of the SpCas9 protein alone is not enough to process the primary transcript, and that ribozyme sequences are necessary to generate functional gRNAs in vitro.

Next, to ensure that both SpCas9 protein and RNase are required to produce functional gRNAs from primary transcribed RNA, we conducted an in vitro DNA cleavage assay using SpCas9:fra–gRNA (Supplementary Fig. S7B) and different combinations of SpCas9 protein and RNases (**Fig. 5**). RNase III and RNase T1 were used as endoribonucleases; when RNase III or RNase T1 were added together with SpCas9 protein, DNA can be cleaved (**Fig. 5**). However, the DNA cleavage efficiency in SpCas9:fra–gRNA was lower than that with OsU6gRNA_T7, 2 × 35SgRNA_T7 or SpCas9:fra–rz–gRNA (**Fig. 5**). When the target sequence was changed, similar results were obtained (Supplementary Fig. S8). These results indicate that functional gRNAs are generated from the RNA of SpCas9:fra–gRNA by the combined action of SpCas9 protein and RNases such as RNase III and RNase T1.

Multiplex targeted mutagenesis using SpCas9–gRNAs vectors

We demonstrated above that no special processing device is needed to generate functional gRNAs for the SpCas9–gRNA system driven by a single pol II promoter in plants. To investigate whether the SpCas9–gRNA system can be applied to multiplex targeted mutagenesis, where targeted mutagenesis occurs independently at multiple sites of the genome, we designed eight multi-gRNA vectors with or without different positions of hammerhead ribozyme sequence (**Fig. 6A**; Supplementary Fig. S9A). In all eight vectors, mutations at both gDL-1 and gDL-2 sites were induced in almost all transgenic calli (**Fig. 6B**; Supplementary Fig. S9A). The mutation frequency in callus line #3 expressing the rz–gDL-1–rz–gDL-2 vector was 75% and 81.2% at gDL-1 and gDL-2 sites, respectively (**Fig. 6B**). The mutation frequencies of callus line #1 expressing the gDL-1–gDL-2 vector were 68.7% and 93.7% at gDL-1 and gDL-2 sites, respectively (**Fig. 6B**). These results indicate that the efficiency of multiplex targeted mutagenesis of SpCas9–gRNAs vectors is comparable with that of SpCas9–rz–gRNA vectors with ribozyme sequence, and that mutation efficiency is not affected by the position of gRNAs. Because target sites gDL-1 and gDL-2 are both located in the same gene, any 1,145 bp deletions between the two target sites can be detected by PCR using primers F1 and R1 (Supplementary Fig. S9B). Using both vectors, several transgenic lines showed small PCR products, meaning that deletion between the two target sites had occurred (Supplementary Fig. S9C). Callus line #2 expressing the gDL-1–gDL-2 vector-transformed calli contained identical gRNA-mediated deletions and junction sequences at the two target sites (Supplementary Fig. S9D). We examined the genotype and phenotype of regenerated plants from transformed calli expressing rz–gDL-1–rz–gDL-2, rz–gDL-2–rz–gDL-1, gDL-1–gDL-2 or gDL-2–gDL-1 vectors. For all four vectors, almost all regenerated plants showed the drooping leaves phenotype, and several mutated plants harbored a deletion of approximately 1,145 bp between the gDL-1 and gDL-2 loci (Supplementary Table S1). These results suggest that the SpCas9–gRNA system can be applied to multiplex targeted mutagenesis.

Discussion

When gRNA is transcribed by a pol III promoter, the resulting poly(T) sequence is used as a termination signal. In this scenario, the four repeated thymines in the gRNA scaffold could potentially disturb gRNA function and reduce the efficiency of targeted mutagenesis in human cells (Dang et al. 2015). However, any negative effect of thymine repeats can be avoided by transcribing the gRNA from an RNA pol II promoter.

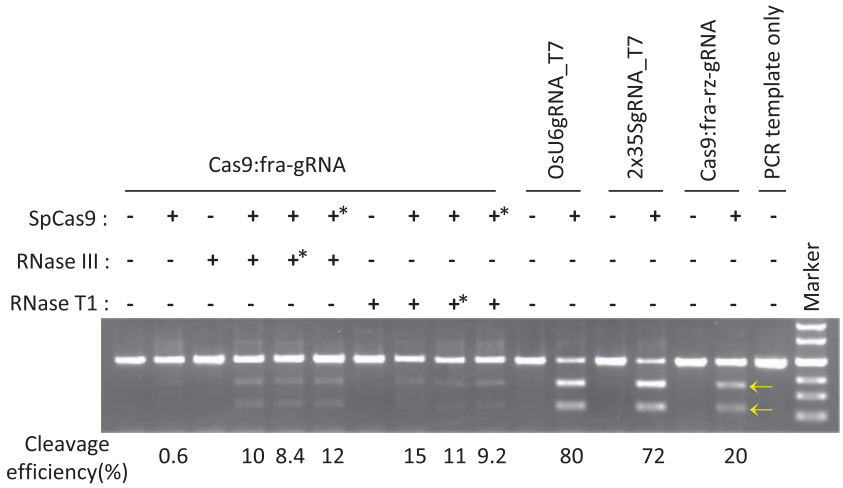

Fig. 5 SpCas9 protein- and RNase(s)-mediated target DNA cleavage in vitro. Cleavage efficiency of the linear target DNA of the gDL-1 locus in an SpCas9 protein- and RNase III- or RNase T1-dependent manner. Yellow arrows indicate the position of cleaved PCR products. Cleavage efficiency was determined by the formula, $100 \times \{1 - \mathrm{sqrt}[1 - (b + c)/(a + b + c)]\}$, where a is the integrated intensity of the PCR product digested only with gRNA, and b and c are the integrated intensities of each cleavage product. +* indicates that the SpCas9 protein, RNase III or RNase T1 were added 20 min after onset of the in vitro cleavage reaction.

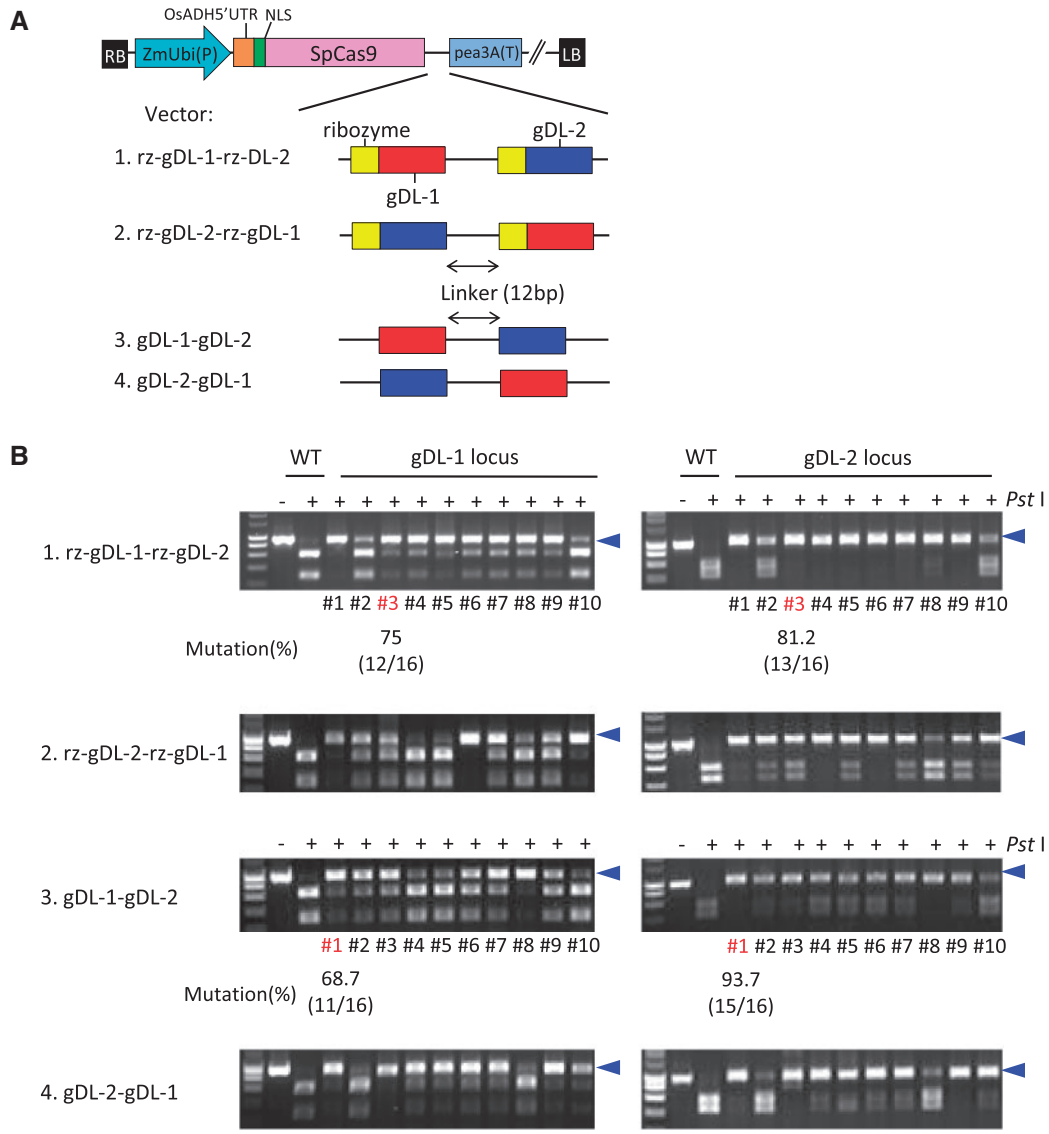

Fig. 6 Multiplex targeted mutagenesis using the SpCas9–gRNA system. (A) Schematic representation of the four multi-gRNA vectors used in this study. Another four vectors are shown in **Supplementary Fig. S9A**. (B) CAPS analysis of the *DL* gene in each of the SpCas9–gRNA vector-transformed calli. The mutation frequency of calli (shown in red) was calculated from the ratio of sequenced clones with mutation. –, non-digested PCR products; +, *Pst* I-digested PCR products. A blue arrowhead indicates the position of undigested PCR products. An undigested band indicates mutations in the target loci.

There are several successful CRISPR/Cas9 reports in which the 35S promoter is used for gRNA expression, for example in wheat (Upadhyay et al. 2013) and sweet orange (Jia and Wang 2014), but the efficiency of targeted mutagenesis was not very high, presumably due to the low activity of unprocessed pol II-expressed gRNAs (Upadhyay et al. 2013). However, we demonstrated here that it is possible to achieve CRISPR/Cas9-mediated mutations with high efficiency when expressing gRNA under the 2 × 35S promoter in rice (**Fig. 2**). Using pol II promoters adds a 5′-cap structure and a 3′-poly(A) tail sequence to the gRNA sequence, producing a longer gRNA than that driven by a pol III promoter. In our study, the 2 × 35SgRNA was 259 nt without the 3′-poly(A) tail sequence, and the gRNA was elongated at the 3′ end (**Fig. 3**). The 2 × 35SgRNA (band *b*) with the 3′-poly(A) tail sequence must have been functional because we showed that mutations were detected with high efficiently in SpCas9/2 × 35SgRNA vector-transformed calli (**Figs. 2**, **3**). Thus, our dual pol II promoter system, avoiding the use of pol III promoters, will be a powerful tool for CRISPR/Cas9-mediated targeted mutagenesis in rice.

This study has demonstrated that SpCas9 protein and intrinsic RNase in plants can produce functional gRNA from a fused SpCas9–gRNA primary transcript. We speculate that this RNA processing mechanism resembles the maturation system of active crRNAs in bacteria and archaea. In native CRISPR/Cas systems, maturation of active crRNAs from the pre-crRNA is critical for the activity of the RNA-guided immunity system that protects bacteria and archaea against phages and plasmids (Brouns et al. 2008, Carte et al. 2008). In the type II CRISPR/Cas9 system, a tracrRNA directs a first processing event of the

pre-crRNA by housekeeping RNase III-mediated cleavage within the CRISPR repeats in the presence of SpCas9 protein (Deltcheva et al. 2011, Chylinski et al. 2013). Then, mature crRNAs are generated by the second processing system of the pre-crRNA, and an exo- or endonuclease seems to be involved in the production of mature crRNAs (Deltcheva et al. 2011, Chylinski et al. 2013, Karvelis et al. 2013, Charpentier et al. 2015). Endogenous RNase III is known to cleave double-stranded RNA to produce different classes of mature RNAs, small nclear RNA (snRNA), small nucleoar RNA (snoRNA), short interfering RNAs (siRNAs) and microRNAs (miRNAs) in both animals and plants (MacRae and Doudna 2007), and thus the notion that plant endogenous RNases can effect gRNA processing is not surprising. To verify this possibility, we conducted in vitro RNA cleavage assays and found that SpCas9 protein and RNases were needed for processing of functional gRNA (**Fig. 5**). Northern blot experiments with SpCas9–rz–gRNA vector- and SpCas9–gRNA vector-transformed calli detected the same two bands (**Fig. 3B**, bands *c* and *d*). Because no signals around 258 nt were detected in GFP/HPT–rz–gRNA-transformed calli (**Fig. 4D**), the self-processing efficiency of the hammerhead ribozyme in rice calli seems low. Thus, band *c* (~332 nt) detected in **Fig. 2B** probably represents a gRNA 5′ end processed by endogenous plant RNases and SpCas9 protein. Band *d*, almost the same size as OsU6gRNA (band *a*), may be a 3′ end processed by exo- or endonucleases, similar to the second processing of pre-crRNA in the native CRISPR/Cas system. These results suggest that SpCas9 protein binds to pol II-transcribed RNA containing the gRNA sequence, with functional gRNAs subsequently being generated by an endogenous RNase(s)-dependent RNA processing system. Actually, a long exposure image of **Fig. 3B** revealed an additional small band that was almost the same size as the band detected in OsU6gRNA (band *a*) in 2 × 35SgRNA (band *d*; Supplementary Fig. S4). We consider that this small RNA was the result of 3′-poly(A) tail sequence cleavage by SpCas9 protein and endogenous RNase, as the same gRNA cleavage occurred in SpCas9–gRNA and SpCas9–rz–gRNA. Future work will be needed to reveal the structure and sequence of gRNAs generated by the endogenous RNase(s)-dependent RNA processing system, perhaps revealing sophisticated gRNA conformations specifically required for plant genome editing.

Several recent reports describe successful CRISPR/Cas9-mediated targeted mutagenesis using ribozyme, Csy4 and tRNA processing systems as processing devices for generating functional gRNAs (Raitskin and Patron 2015, Lowder et al. 2016, Schwartz et al. 2016, Cermak et al. 2017). In a single transcript unit system in which both SpCas9 and gRNA were expressed from a single pol II promoter, high levels of CRISPR/Cas9-mediated targeted mutagenesis efficiency (up to 100%) were achieved by the ribozyme and tRNA processing systems in rice (Xie et al. 2015, Minkenberg et al. 2016, Tang et al. 2016). However, in these latter studies the ribozyme requires 43 bp, and Csy4 and tRNA require 20 and 77 bp, respectively, to separate individual functional gRNAs from the transcript. In our ribozyme-independent SpCas9–gRNA system, targeted mutagenesis efficiencies using single and multi-gRNAs were also both close to 100% in rice (**Figs. 1**, **6**; Supplementary Table S1).

One effective use of our ribozyme-independent gRNA expression system may be in RNA virus vector-mediated genome editing. RNA virus-based replicons have been tested as vectors for delivery of CRISPR components to produce a high incidence of edited cells without the incorporation of recombinant DNA (Ali et al. 2015, Kaya et al. 2017). In general, adjustment of replication of the RNA virus vector and retention of the amount of functional gRNA are balanced by the activity of ribozyme. However, ribozymes, especially the hammerhead ribozyme, flanking the 5′ end of the gRNA, have been shown to have a negative effect on the replication of *Tobacco mosaic virus*-derived vector (TRBO) (Cody et al. 2017). A system supplying ribozyme-free gRNA could stabilize replication of an RNA virus vector; indeed, a TRBO–gRNA expression vector without ribozyme sequence supplied functional gRNA in *Nicotiana benthamiana*. (Cody et al. 2017). Our present study provides new insights into the current understanding of gRNA supply in vivo, and our findings illustrate new features of smaller and stable systems for expressing SpCas9 and gRNA in plants.

Materials and Methods

Construction of SpCas9–rz–gRNA and SpCas9–gRNA vectors

The SpCas9–rz–gRNA and SpCas9–gRNA vectors used in this study were based on our previously described SpCas9 cloning vectors (pZH_MMCas9; Mikami et al. 2015). To add the hammerhead ribozyme sequence and gRNA next to the SpCas9 sequence, we added *Nco* I and *Spe* I sites between SpCas9 and pea3A(T) by PCR-based site-directed mutagenesis. The SpCas9–rz–gRNA and SpCas9–gRNA vectors were constructed as follows: (i) the pUC19_gRNA [*Nco* I::gRNA scaffold::polyT::*Spe* I] vector has two *Bbs* I sites between the *Nco* I site and the gRNA scaffold sequence. This vector was linearized using *Bbs* I, and the 67 nt (hammerhead ribozyme sequence::target sequence) or 24 nt (target sequence) annealed oligonucleotides were ligated into the *Bbs*I site (Supplementary Table S2). (ii) Connected ribozyme–gRNA (rz–gRNA) or gRNA-coding sequences were excised from the pUC19_gRNA vector using *Nco* I and *Spe*I digestion, and inserted into the pZH_ZmUbi-SpCas9 vector using *Nco* I and *Spe* I to complete the SpCas9–rz–gRNA and SpCas9–gRNA constructs. (iii) To create SpCas9–rz–gRNA and SpCas9–gRNA vectors with 2 × 35S, PcUbi and G10-90 promoters, the ZmUbi promoter located between *Asc*I and *Xba*I was eliminated and replaced by other promoters.

Construction of SpCas9/2 × 35SgRNA vector

The SpCas9/2 × 35SgRNA vector is based on previously described SpCas9 cloning vectors (pZH_p-gRNA_MMCas9-Nuclease; Mikami et al. 2016). The SpCas9/2 × 35SgRNA vector was constructed as follows: (i) the p2 × 35SgRNA [2 × 35S(P)::gRNA scaffold::polyT::35S(T)] vector has two *Bsa* I sites between the 2 × 35S promoter and the gRNA scaffold sequence. This vector was digested by *Bsa* I, and 20 nt annealed oligonucleotides were ligated into the cleaved site to insert the required target sequence (Supplementary Table S2). (ii) gRNA expression cassettes were excised from the p2 × 35SgRNA vector using *Asc* I and *Pac* I digestion, and inserted into the pZH_p-gRNA_MMCas9-Nuclease vector using *Asc* I and *Pac* I sites to complete the SpCas9/2 × 35SgRNA vector.

Transformation of rice with SpCas9–gRNA expression constructs

Agrobacterium-mediated transformation of rice (*Oryza sativa* L. cv. Nipponbare) using scutellum-derived calli was performed as described previously (Toki 1997, Toki et al. 2006). Rice calli cultured for 1 month were infected by *Agrobacterium* carrying the CRISPR/Cas9 vectors. After 3 d of co-cultivation,

infected calli were transferred to fresh callus induction medium (CIM) (Toki 1997) containing 50 mg l^{-1} hygromycin B (Wako Pure Chemicals) and 25 mg l^{-1} meropenem (Wako Pure Chemicals) to remove *Agrobacterium*. Transgenic calli were selected on hygromycin-containing medium for 3 weeks. Proliferating calli were then transferred to fresh CIM and cultured for 1 week. After a total of 4 weeks of selection, transgenic calli of the CRISPR/Cas9 vectors were used for analysis of mutation frequency.

CRISPR/Cas9-mediated mutation analysis

Genomic DNA was extracted from calli or regenerated plants using an Agencourt Chloropure Kit (Beckman Coulter), and target loci were amplified using the primers listed in Supplementary Table S2. PCR products were subjected to restriction enzyme digestion and CAPS analysis, and analyzed by agarose gel electrophoresis.

Sequencing analysis

PCR products used for CAPS analysis were cloned into pCR-BluntII-TOPO (Invitrogen) and subjected to sequence analysis using an ABI3130 sequencer (Applied Biosystems).

Northern blot analysis of gRNA in rice calli

Total RNA was extracted from calli using the mirVana small RNA isolation kit (Ambion). For each sample, 10 μg of total RNA was separated on a 10% urea–polyacrylamide gel after denaturation for 2 min at 95°C. After electrophoresis for 100 min at 200 V in 1 × TBE buffer, samples were electroblotted onto a positively charged nylon membrane (Roche) at 20 V for 90 min in 1 × TBE buffer. The transferred RNAs were pre-hybridized at 50°C for 2 h in hybridization buffer [5 × SSC, 50% formamide, 0.1% *N*-lauroylsarcosine, 7% SDS, 50 mM sodium phosphate (pH 7.0), 2% blocking reagent (Roche)]. The pre-hybridized membranes were incubated overnight in hybridization buffer supplemented with Custom LNA mRNA Detection probe (/5DigN/AAGTTGATAACGGACTAGCCT/3Dig_N/; EXIQON) at 10 nM. After several washes in SSC buffer (final wash in 0.2 × SSC), Northern blot hybridization signals of gRNA were detected and analyzed using a ChemiDoc Touch Imaging System (Bio-Rad). Marker-1, RNA Molecular Weight Marker I, DIG-labeled (Roche); Marker-2, DynaMarker, DIG-Labeled Blue Color Marker for Small RNA (FunakoshI).

In vitro cleavage assay

OsU6gRNA_T7 was synthesized using a Guide-it sgRNA In vitro Transcription Kit (TAKARA). Other in vitro transcribed gRNAs were synthesized using an in vitro Transcription T7 Kit (TAKARA). Target DNA was amplified from plasmid DNA using the primers listed in Supplementary Table S2, and a short T7 priming sequence was added to the amplified target DNA. T7 transcription was performed for 4 h, and the synthesized gRNAs were then purified using a NucleoSpin RNA Clean-up Kit (TAKARA). Cleavage was performed in vitro according to the Guide-it sgRNA Screening Kit (TAKARA). The cleavage reaction used 500 ng of Guide-it Recombinant Cas9 Nuclease (TAKARA), 100 ng of synthesized gRNA and 100 ng of linear target DNA. Also, 0.5 U of RNase III (New England Biolabs) or 0.02 U of RNase T1 (Thermo Fisher Scientific) were added and incubated for 60 min at 37°C. The reaction was stopped by incubating for 10 min at 70°C. For analysis of DNA cleavage efficiency and Northern blot, the reaction solution was divided in half; to one half was added RNase A (QIAGEN) and proteinase K (TAKARA), and to the other DNase I (QIAGEN) and proteinase K (TAKARA).

Supplementary data

Supplementary data are available at PCP online.

Funding

This research was supported by the Bio-oriented Technology Research Advancement Institution, NARO [a grant from the Cross-ministerial Strategic Innovation Promotion Program (SIP); Technologies for creating next-generation agriculture, forestry and fisheries] and the Japan Society for the Promotion of Science [Research Fellowship for Young Scientists (grant No. 16J06425 to M.M.]

Acknowledgments

We thank K. Amagai, R. Aoto, A. Nagashii F. Suzuki, R. Takahashi and C. Furusawa for general experimental technical support.

Disclosures

The authors have no conflicts of interest to declare.

References

Ali, Z., Abul-faraj, A., Li, L., Ghosh, N., Piatek, M., Mahjoub, A., et al. (2015) Efficient virus-mediated genome editing in plants using the CRISPR/Cas9 System. *Mol. Plant* 8: 1288–1291.

Barbezier, N., Canino, G., Rodor, J., Jobet, E., Saez-Vasquez, J., Marchfelder, A., et al. (2009) Processing of a dicistronic tRNA–snoRNA precursor: combined analysis in vitro and in vivo reveals alternate pathways and coupling to assembly of snoRNP. *Plant Physiol.* 150: 1598–1610.

Bortesi, L. and Fischer, R. (2015) The CRISPR/Cas9 system for plant genome editing and beyond. *Biotechnol. Adv.* 33: 41–52.

Brouns, S.J., Jore, M.M., Lundgren, M., Westra, E.R., Slijkhuis, R.J., Snijders, A.P., et al. (2008) Small CRISPR RNAs guide antiviral defense in prokaryotes. *Science* 321: 960–964.

Canino, G., Bocian, E., Barbezier, N., Echeverria, M., Forner, J., Binder, S., et al. (2009) Arabidopsis encodes four tRNase Z enzymes. *Plant Physiol.* 150: 1494–1502.

Carte, J., Wang, R., Li, H., Terns, R.M. and Terns, M.P. (2008) Cas6 is an endoribonuclease that generates guide RNAs for invader defense in prokaryotes. *Genes Dev.* 22: 3489–3496.

Cermak, T., Curtin, S.J., Gil-Humanes, J., Cegan, R., Kono, T.J.Y., Konecna, E., et al. (2017) A multi-purpose toolkit to enable advanced genome engineering in plants. *Plant Cell.* 29: 1196–1217.

Charpentier, E., Richter, H., van der Oost, J. and White, M.F. (2015) Biogenesis pathways of RNA guides in archaeal and bacterial CRISPR–Cas adaptive immunity. *FEMS Microbiol. Rev.* 39: 428–441.

Cho, S.W., Kim, S., Kim, J.M. and Kim, J.S. (2013) Targeted genome engineering in human cells with the Cas9 RNA-guided endonuclease. *Nat. Biotechnol.* 31: 230–232.

Chylinski, K., Le Rhun, A. and Charpentier, E. (2013) The tracrRNA and Cas9 families of type II CRISPR-Cas immunity systems. *RNA Biol.* 10: 726–737.

Cody, W., Scholthof, H.B. and Mirkov, T.E. (2017) Multiplexed gene editing and protein over-expression using a Tobacco mosaic virus viral vector. *Plant Physiol.* 175: 23–35.

Condon, C. (2007) Maturation and degradation of RNA in bacteria. *Curr. Opin. Microbiol.* 10: 271–278.

Cong, L., Ran, F.A., Cox, D., Lin, S., Barretto, R., Habib, N., et al. (2013) Multiplex genome engineering using CRISPR/Cas systems. *Science* 339: 819–823.

Dang, Y., Jia, G., Choi, J., Ma, H., Anaya, E., Ye, C., et al. (2015) Optimizing sgRNA structure to improve CRISPR–Cas9 knockout efficiency. *Genome Biol.* 16: 280.

Deltcheva, E., Chylinski, K., Sharma, C.M., Gonzales, K., Chao, Y., Pirzada, Z.A., et al. (2011) CRISPR RNA maturation by trans-encoded small RNA and host factor RNase III. *Nature* 471: 602–607.

DiCarlo, J.E., Norville, J.E., Mali, P., Rios, X., Aach, J. and Church, G.M. (2013) Genome engineering in *Saccharomyces cerevisiae* using CRISPR–Cas systems. *Nucleic Acids Res.* 41: 4336–4343.

Drider, D. and Condon, C. (2004) The continuing story of endoribonuclease III. *J. Mol. Microbiol. Biotechnol.* 8: 195–200.

Fauser, F., Roth, N., Pacher, M., Ilg, G., Sanchez-Fernandez, R., Biesgen, C., et al. (2012) In planta gene targeting. *Proc. Natl. Acad. Sci. USA* 109: 7535–7540.

Fauser, F., Schiml, S. and Puchta, H. (2014) Both CRISPR/Cas-based nucleases and nickases can be used efficiently for genome engineering in *Arabidopsis thaliana*. *Plant J.* 79: 348–359.

Gao, Y., Zhang, Y., Zhang, D., Dai, X., Estelle, M. and Zhao, Y. (2015) Auxin binding protein 1 (ABP1) is not required for either auxin signaling or Arabidopsis development. *Proc. Natl. Acad. Sci. USA* 112: 2275–2280.

Gao, Y. and Zhao, Y. (2014) Self-processing of ribozyme-flanked RNAs into guide RNAs in vitro and in vivo for CRISPR-mediated genome editing. *J. Integr. Plant Biol.* 56: 343–349.

Gutmann, B., Gobert, A. and Giege, P. (2012) PRORP proteins support RNase P activity in both organelles and the nucleus in Arabidopsis. *Genes Dev.* 26: 1022–1027.

Haurwitz, R.E., Jinek, M., Wiedenheft, B., Zhou, K. and Doudna, J.A. (2010) Sequence- and structure-specific RNA processing by a CRISPR endonuclease. *Science* 329: 1355–1358.

Hsu, P.D., Scott, D.A., Weinstein, J.A., Ran, F.A., Konermann, S., Agarwala, V., et al. (2013) DNA targeting specificity of RNA-guided Cas9 nucleases. *Nat. Biotechnol.* 31: 827–832.

Hwang, W.Y., Fu, Y., Reyon, D., Maeder, M.L., Kaini, P., Sander, J.D., et al. (2013) Heritable and precise zebrafish genome editing using a CRISPR–Cas system. *PLoS One* 8: e68708.

Ishige, F., Takaichi, M., Foster, R., Chua, N.H. and Oeda, K. (1999) A G-box motif (GCCACGTGCC) tetramer confers high-level constitutive expression in dicot and monocot plants. *Plant J.* 18: 443–448.

Jia, H. and Wang, N. (2014) Targeted genome editing of sweet orange using Cas9/sgRNA. *PLoS One* 9: e93806.

Jiang, W., Bikard, D., Cox, D., Zhang, F. and Marraffini, L.A. (2013) RNA-guided editing of bacterial genomes using CRISPR–Cas systems. *Nat. Biotechnol.* 31: 233–239.

Jinek, M., Chylinski, K., Fonfara, I., Hauer, M., Doudna, J.A. and Charpentier, E. (2012) A programmable dual-RNA-guided DNA endonuclease in adaptive bacterial immunity. *Science* 337: 816–821.

Jinek, M., East, A., Cheng, A., Lin, S., Ma, E. and Doudna, J. (2013) RNA-programmed genome editing in human cells. *Elife* 2: e00471.

Karvelis, T., Gasiunas, G., Miksys, A., Barrangou, R., Horvath, P. and Siksnys, V. (2013) crRNA and tracrRNA guide Cas9-mediated DNA interference in *Streptococcus thermophilus*. *RNA Biol.* 10: 841–851.

Kaya, H., Ishibashi, K. and Toki, S. (2017) A split *Staphylococcus aureus* Cas9 as a compact genome-editing tool in plants. *Plant Cell Physiol* 58: 643–649.

Li, J.F., Norville, J.E., Aach, J., McCormack, M., Zhang, D., Bush, J., et al. (2013) Multiplex and homologous recombination-mediated genome editing in Arabidopsis and *Nicotiana benthamiana* using guide RNA and Cas9. *Nat. Biotechnol.* 31: 688–691.

Lowder, L., Malzahn, A. and Qi, Y. (2016) Rapid evolution of manifold CRISPR systems for plant genome editing. *Front. Plant Sci.* 7: 1683.

Ma, X., Zhu, Q., Chen, Y. and Liu, Y.G. (2016) CRISPR/Cas9 platforms for genome editing in plants: developments and applications. *Mol. Plant* 9: 961–974.

MacRae, I.J. and Doudna, J.A. (2007) Ribonuclease revisited: structural insights into ribonuclease III family enzymes. *Curr. Opin. Struct. Biol.* 17: 138–145.

Mali, P., Aach, J., Stranges, P.B., Esvelt, K.M., Moosburner, M., Kosuri, S., et al. (2013) CAS9 transcriptional activators for target specificity screening and paired nickases for cooperative genome engineering. *Nat. Biotechnol.* 31: 833–838.

Mikami, M., Toki, S. and Endo, M. (2015) Comparison of CRISPR/Cas9 expression constructs for efficient targeted mutagenesis in rice. *Plant Mol. Biol.* 88: 561–572.

Mikami, M., Toki, S. and Endo, M. (2016) Precision targeted mutagenesis via Cas9 paired nickases in rice. *Plant Cell Physiol.* 57: 1058–1068.

Minkenberg, B., Xie, K. and Yang, Y. (2016) Discovery of rice essential genes by characterizing CRISPR-edited mutation of closely related rice MAP kinase genes. *Plant J.* 83: 636–648.

Nekrasov, V., Staskawicz, B., Weigel, D., Jones, J.D. and Kamoun, S. (2013) Targeted mutagenesis in the model plant *Nicotiana benthamiana* using Cas9 RNA-guided endonuclease. *Nat. Biotechnol.* 31: 691–693.

Nicholson, A.W. (1999) Function, mechanism and regulation of bacterial ribonucleases. *FEMS Microbiol. Rev.* 23: 371–390.

Nissim, L., Perli, S.D., Fridkin, A., Perez-Pinera, P. and Lu, T.K. (2014) Multiplexed and programmable regulation of gene networks with an integrated RNA and CRISPR/Cas toolkit in human cells. *Mol. Cell* 54: 698–710.

Phizicky, E.M. and Hopper, A.K. (2010) tRNA biology charges to the front. *Genes Dev.* 24: 1832–1860.

Raitskin, O. and Patron, N.J. (2015) Multi-gene engineering in plants with RNA-guided Cas9 nuclease. *Curr. Opin. Biotechnol.* 37: 69–75.

Sakane, I., Kamataki, C., Takizawa, Y., Nakashima, M., Toki, S., Ichikawa, H., et al. (2008) Filament formation and robust strand exchange activities of the rice DMC1A and DMC1B proteins. *Nucleic Acids Res.* 36: 4266–4276.

Schiffer, S., Rosch, S. and Marchfelder, A. (2002) Assigning a function to a conserved group of proteins: the tRNA 3′-processing enzymes. *EMBO J.* 21: 2769–2777.

Schwartz, C.M., Hussain, M.S., Blenner, M. and Wheeldon, I. (2016) Synthetic RNA polymerase III promoters facilitate high-efficiency CRISPR–Cas9-mediated genome editing in *Yarrowia lipolytica*. *ACS Synth. Biol.* 5: 356–359.

Shan, Q., Wang, Y., Li, J., Zhang, Y., Chen, K., Liang, Z., et al. (2013) Targeted genome modification of crop plants using a CRISPR–Cas system. *Nat. Biotechnol.* 31: 686–688.

Takimoto, I., Christensen, A.H., Quail, P.H., Uchimiya, H. and Toki, S. (1994) Non-systemic expression of a stress-responsive maize polyubiquitin gene (Ubi-1) in transgenic rice plants. *Plant Mol. Biol.* 26: 1007–1012.

Tang, X., Zheng, X., Qi, Y., Zhang, D., Cheng, Y., Tang, A., et al. (2016) A single transcript CRISPR–Cas9 system for efficient genome editing in plants. *Mol. Plant* 9: 1088–1091.

Toki, S. (1997) Rapid and efficient Agrobacterium-mediated transformation in rice. *Plant Mol. Biol. Rep.* 15: 16–21.

Toki, S., Hara, N., Ono, K., Onodera, H., Tagiri, A., Oka, S., et al. (2006) Early infection of scutellum tissue with Agrobacterium allows high-speed transformation of rice. *Plant J.* 47: 969–976.

Tsai, S.Q., Wyvekens, N., Khayter, C., Foden, J.A., Thapar, V., Reyon, D., et al. (2014) Dimeric CRISPR RNA-guided FokI nucleases for highly specific genome editing. *Nat. Biotechnol.* 32: 569–576.

Upadhyay, S.K., Kumar, J., Alok, A. and Tuli, R. (2013) RNA-guided genome editing for target gene mutations in wheat. *G3 (Bethesda)* 3: 2233–2238.

Xie, K., Minkenberg, B. and Yang, Y. (2015) Boosting CRISPR/Cas9 multiplex editing capability with the endogenous tRNA-processing system. *Proc. Natl. Acad. Sci. USA* 112: 3570–3575.

Yamaguchi, T., Nagasawa, N., Kawasaki, S., Matsuoka, M., Nagato, Y. and Hirano, H.Y. (2004) The YABBY gene DROOPING LEAF regulates carpel specification and midrib development in *Oryza sativa*. *Plant Cell* 16: 500–509.

Yoshioka, S., Fujii, W., Ogawa, T., Sugiura, K. and Naito, K. (2015) Development of a mono-promoter-driven CRISPR/Cas9 system in mammalian cells. *Sci. Rep.* 5: 18341.